Electronic Supplementary Material (ESI)

Coordinatively Unsaturated 5-Nitroisophthalate based Cobalt(II) Coordination Polymers: Efficient Catalytic CO_2 Fixation and Hantzsch Condensation

*Subham Sahoo[1], Rajesh Patra[1], and Debajit Sarma[1]**

[1]Department of Chemistry, Indian Institute of Technology Patna, Bihar 801106, India

*E-mail: debajit@iitp.ac.in

Contents

Materials and methods 3

Experimental section 3

Structural motif 5

Characterization 6

Catalytic CO_2 cycloaddition 7

Table S1. Controlled reaction data for the CO_2 cycloaddition reactions 7

Table S2. Comparison table for CO_2 cycloaddition reaction. 10

Catalytic Hantzsch Condensation 11

Table S3. Controlled reaction data for the Hantzsch condensation reactions[a] 11

Table S4. Comparison table for the catalytic Hantzsch condensation performance. 15

Table S5. Selected Bond Distances (Å) and Bond Angles (°) 15

Table S6. H-bonding interactions 16

References 16

Materials and methods

All the solvents and reagents were purchased from commercial sources and used without further purification. The commercially obtained reagents mentioned above were used without further purification. The single crystal XRD diffraction data was collected using BRUKER AXS (D8 Quest System) X-ray diffractometer. Powder X-Ray diffraction patterns were recorded on PANalytical X'Pert Pro Diffractometer operated at 40 kV and 45 mA with Cu Kα radiation. The surface area measurement analysis was performed by the Quantachrome autosorb iQ2 analyzer. Thermogravimetric analysis was carried out using an SDT Q600 (TA Instruments), and the samples were heated from room temperature to 800°C at 10 °C min^{-1} rate under N_2 gas flow rate of 100 mL/min. ^{1}H NMR spectrum was recorded using a Bruker 400 MHz spectrometer.

Experimental section

Synthesis of 4-ABPT (4-amino-3,5-bis(pyridine-2-yl)-1,2,4-triazole). The ligand was synthesized following the reported procedure.[1] A mixture of 4-cyano pyridine (25mmol), hydrazine monohydrate (80%, 3mL), and ethanol (1mL) were mixed in an autoclave and heated at 120°C for 3 days, followed by slow cooling to room temperature, which results white crystalline substance. The NMR data match with the reported literature. Yield: 90 % (4.75 gm). ^{1}HNMR (400 MHz, DMSO-d_6): δ 8.80 (4H, d, Hc), 8.08 (4H, d, Hb), 6.55 (2H, s, Ha). ^{13}C NMR (400 MHz, DMSO-d_6): δ 153.53 (C1), 150.62 (C4), 139.16 (C2), 122.53 (C3).

Synthesis of [Co(4-ABPT)(NIPA)(H_2O)$_3$], SSICG-6. A mixture of $Co(OAc)_2{\cdot}4H_2O$ (1 mmol), H_2NIPA (1 mmol), and 4-ABPT (1 mmol) was taken in 3 mL of distilled water in a 15 mL screw-capped vial. Then, the mixture was ultrasonicated for 10 min to make it homogeneous and heated to 100 °C for 3 days and then slowly cooled down to room temperature. Purple-colored, block-shaped X-ray quality crystals were obtained, which were then filtered and thoroughly washed with water. Yield: 78 %

Synthesis of [Co(4-ABPT)(NIPA)(H_2O)], SSICG-7. A mixture of $Co(OAc)_2 \cdot 4H_2O$ (1 mmol), H_2NIPA (1 mmol), and 4-ABPT (1 mmol) was taken in 3 mL of distilled water in a 15 mL screw-capped vial. Then, the mixture was stirred for 10 min to make it homogeneous and heated to 150 °C for 3 days and then slowly cooled down to room temperature. Purple-colored, block-shaped X-ray quality crystals were obtained, which were then filtered and thoroughly washed with water. Yield: 68 %

Catalytic CO_2 cycloaddition reactions. The catalytic reactions were carried out in the presence of carbon dioxide (CO_2) at atmospheric pressure (balloon) and under solvent-free conditions at room temperature (rt). 20 mmol epoxide, 2.5 mol% tetrabutylammonium bromide (TBAB) were used as substrate and cocatalyst respectively. ^{1}HNMR of the filtrate was recorded to calculate the conversion.

Hantzsch condensation reaction. In a 10 mL round bottom flask, 1 mmol of aldehyde, 1 mmol of ammonium acetate, and 2 mmol of ethyl acetoacetate were dissolved in 1 mL of ethanol. After adding 2.5 mol% catalyst, the reaction was carried out at 60 °C for 4 h. After completion, the reaction mixture was centrifuged to separate the catalyst. Column chromatography was performed to purify the products and the products were analyzed by ^{1}HNMR.

DFT energy calculation. Ab initio calculations have been carried out using the density functional theory (DFT) exchange-correlation function B3LYP with basis set of 6-311+G*, to optimize the structures of substrate scope and calculate the π- π stabilization energy of the compounds SSICG-6.

Crystallographic data and structure refinements. Good quality single crystal of the compound was sorted out with the help of a polarizing microscope. The single crystal XRD diffraction data was collected using BRUKER AXS (D8 Quest System) X-ray diffractometer, equipped with a PHOTON 100 CMOS detector. Source of X-ray was a Mo Kα (λ = 0.71073 Å) radiation. Bruker

Apex III software was used for data collection, unit cell measurement, absorption corrections, scaling, and integration.[2] The data was reduced, and an empirical absorption correction was applied with the help of SAINTPLUS and SADABS programmes respectively.[3, 4] SHELXL97[5] present in the WinGx (Version 1.63.04a) programs were used to solve the crystal structure. The WinGx package of programmes was used to carry out the full-matrix least-squares refinement against the function $|F^2|$.[6-8] The calculated 'H's are fixed with the help of Olex2-1.5 programme.[7, 8] 'OMIT' command has been used to remove bad reflections. The structure detail of the compound is presented in Table 1. CCDC: 2325939 and 2325940 contains the crystallographic data of these compounds. These data is available from the Cambridge Crystallographic Data Center (CCDC) *via* www.ccdc.cam.ac.uk/data_request/cif.

Structural motif

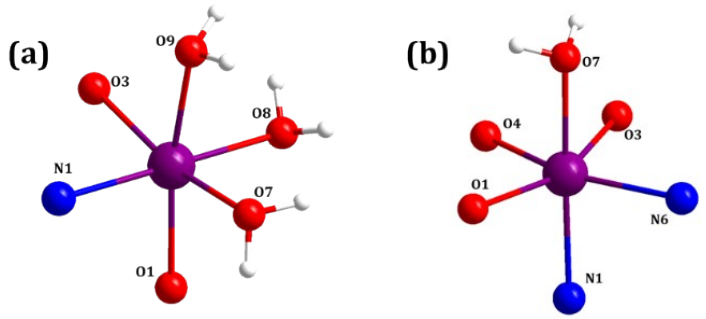

Figure S1. Coordination environment of metal centre in (a) SSICG-6, and (b) SSICG-7.

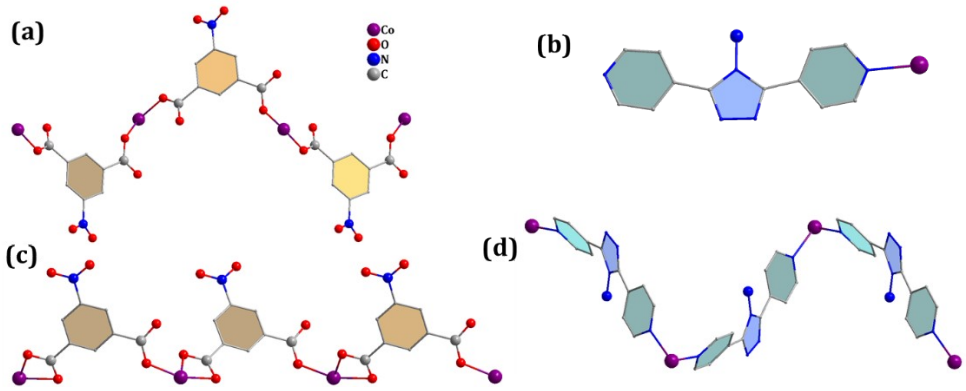

Figure S2. Binding motif of (a) NIPA, (b) 4-ABPT in SSICG-6; and (c) NIPA, (d) 4-ABPT in SSICG-7.

Characterization

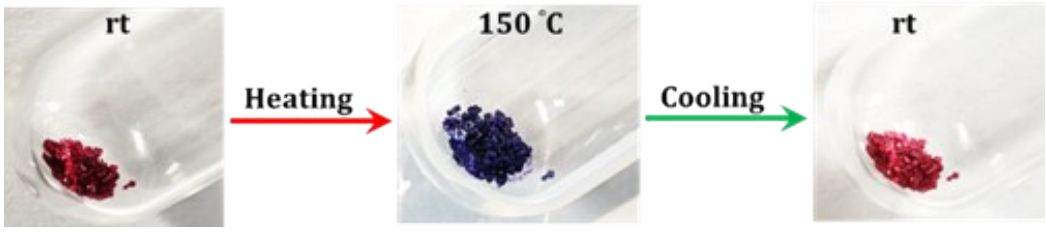

Figure S3. Color change of SSICG-6 on heating at 150 °C and cooling to rt.

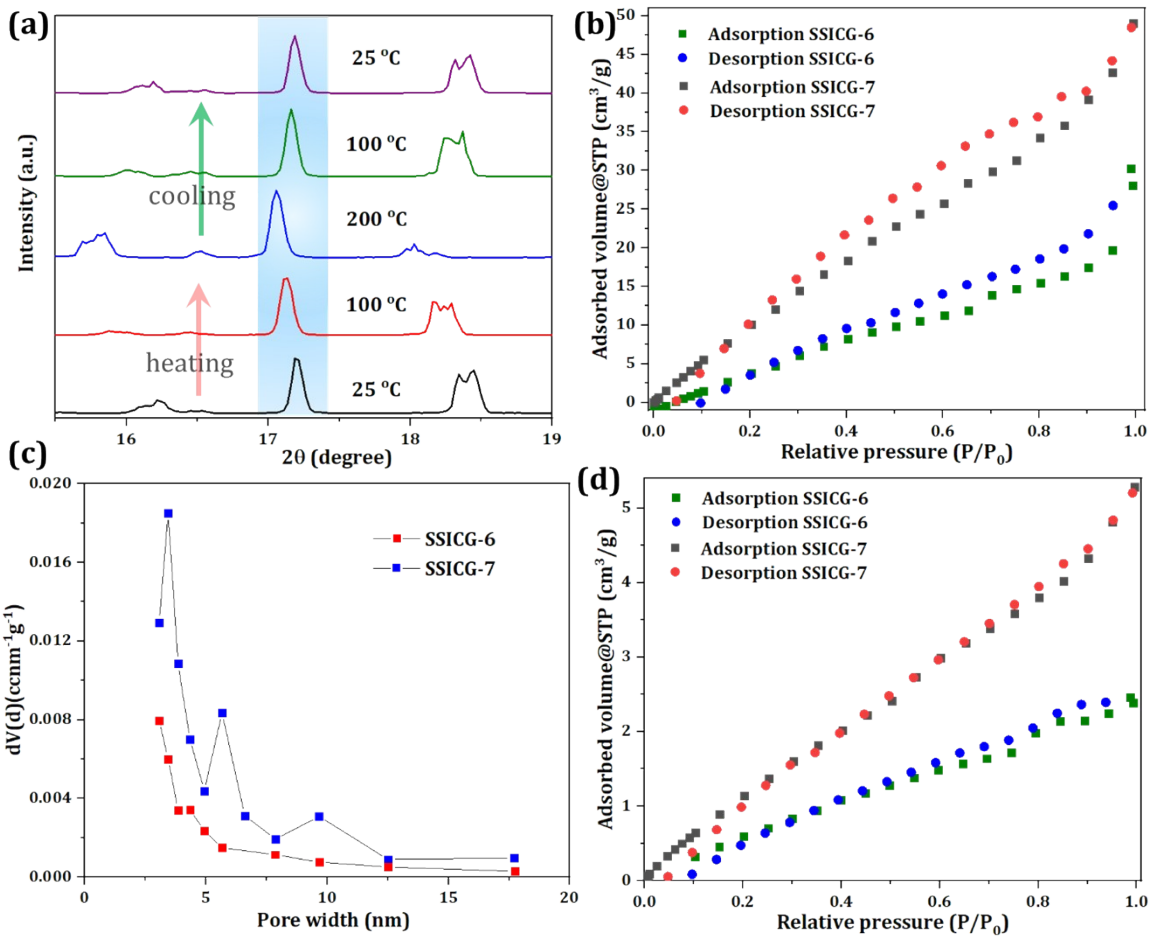

Figure S4. (a) VT-PXRD of SSICG-7, (b) N_2 sorption isotherm at 77K, (c) pore size distribution (PSD) plot, and (d) CO_2 sorption isotherm at 273 K of SSICG-6 and 7.

Catalytic CO_2 cycloaddition

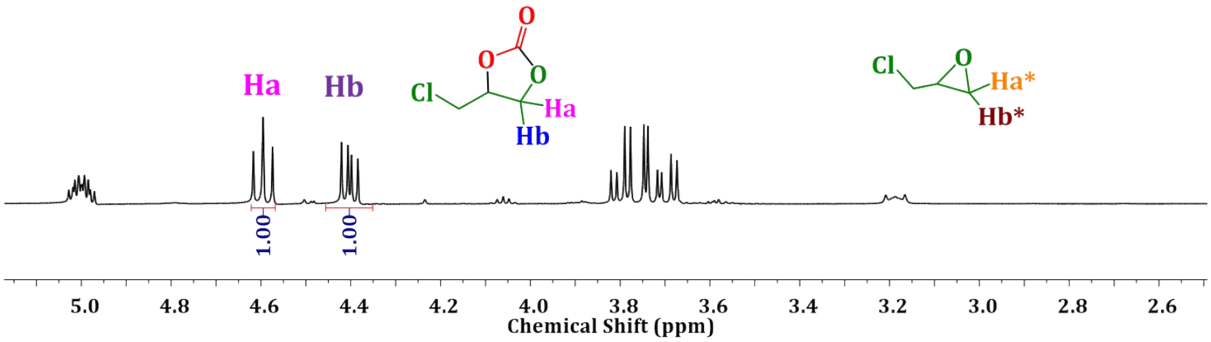

Figure. S5. ^{1}H NMR spectra for the cycloaddition reaction of epichlorohydrin using SSICG-6.

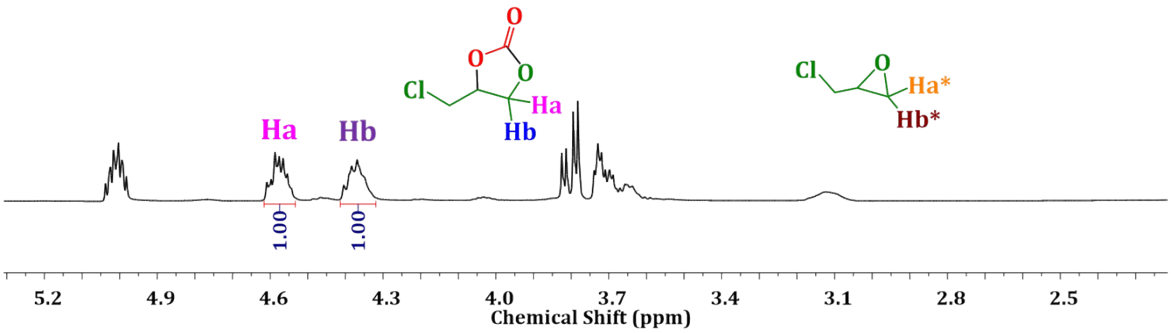

Figure. S6. ^{1}H NMR spectra for the cycloaddition reaction of epichlorohydrin using SSICG-7.

Table S1. Controlled reaction data for the CO_2 cycloaddition reactions

Entry	Catalyst	Conversion[a] (%)
1	$Co(OAc)_2 \cdot 4H_2O$	37
3	H_2NIPA	29
4	4-ABPT	25
5	Without cocatalyst	43
6	Without catalyst	9

(a) Percentage of conversions were determined by ^{1}H NMR analysis.

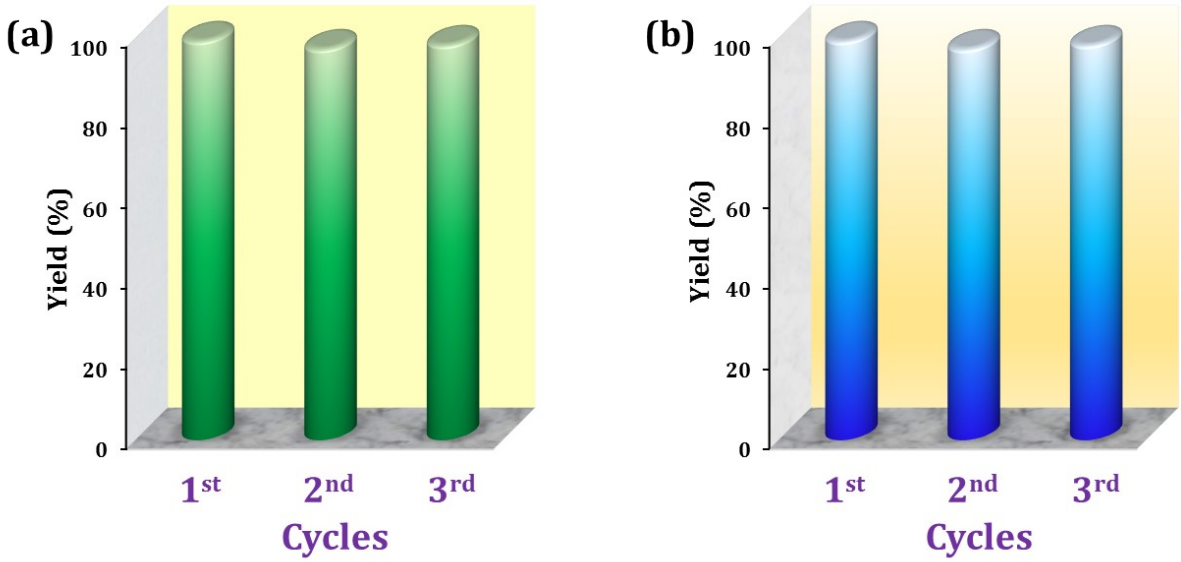

Figure S7. Recyclability test for (a) SSICG-6 and (b) SSICG-7 catalyzed CO_2 cycloaddition reaction up to three cycles.

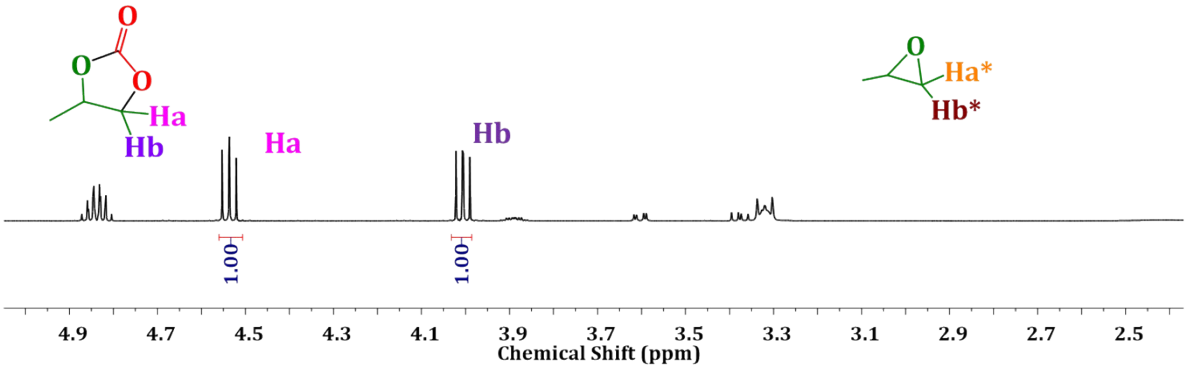

Figure. S8. ^{1}H NMR spectra for the cycloaddition reaction of propylene oxide using SSICG-6.

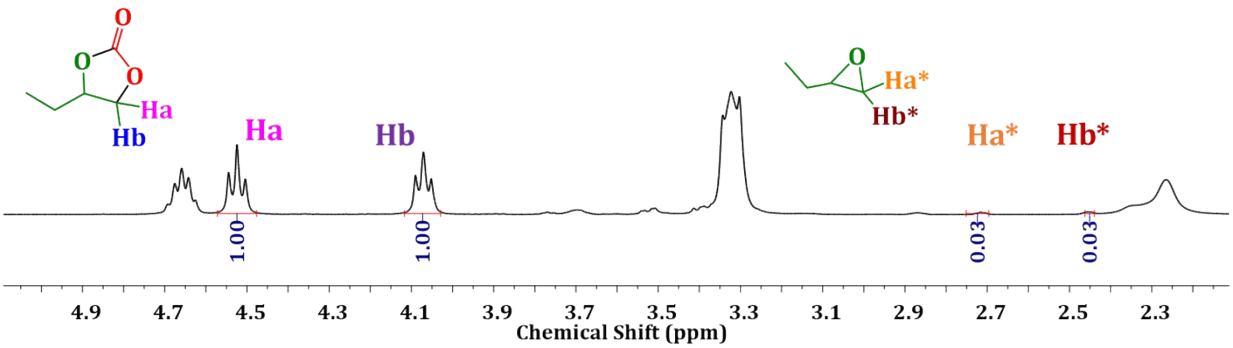

Figure. S9. ^{1}H NMR spectra for the cycloaddition reaction of 1,2-epoxybutane using SSICG-6.

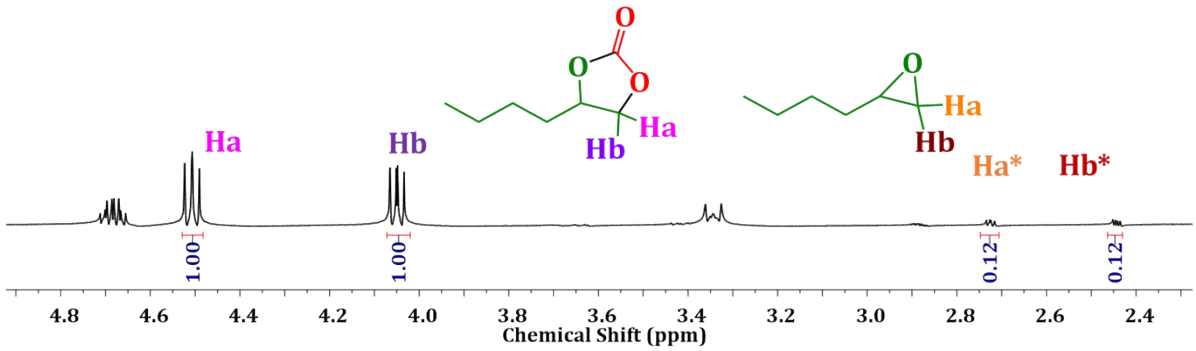

Figure. S10. ^{1}H NMR spectra for the cycloaddition reaction of 1,2-epoxyhexane using SSICG-6.

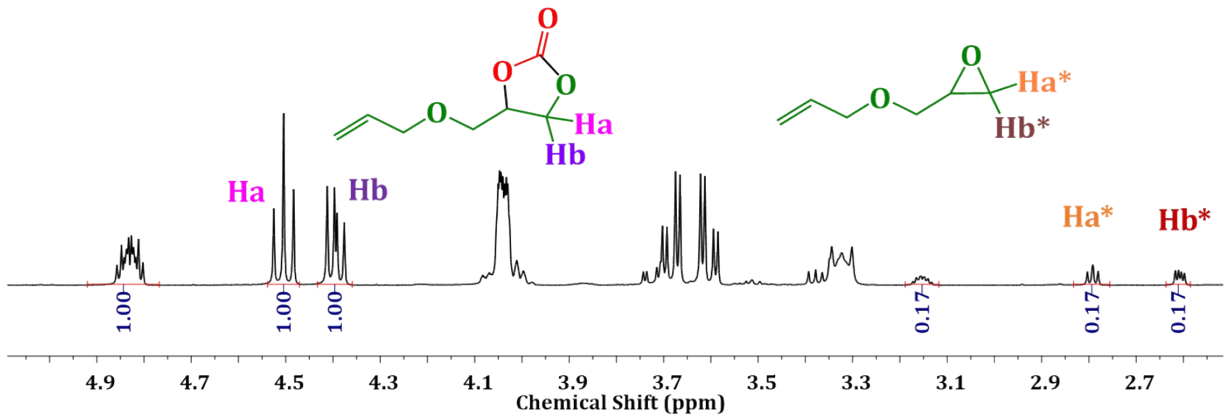

Figure. S11. ^{1}H NMR spectra for the cycloaddition reaction of allyl glycidyl ether using SSICG-6.

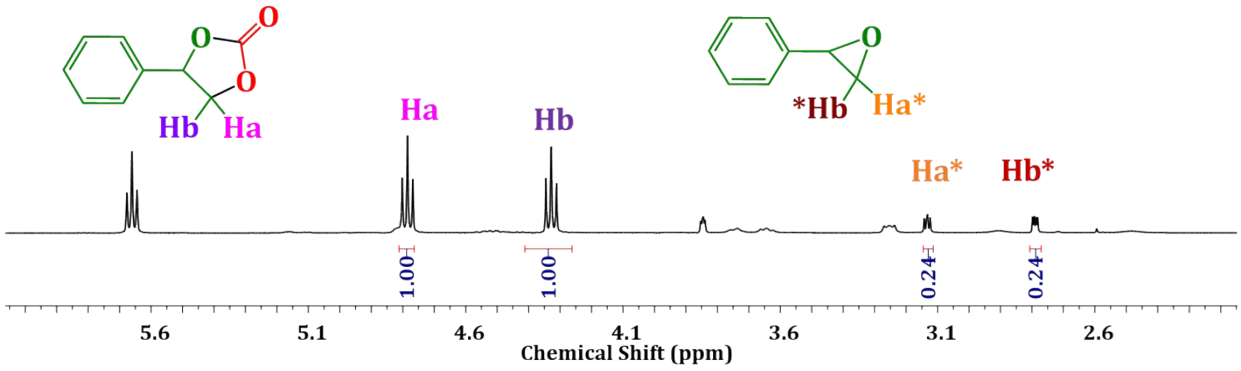

Figure. S12. ^{1}H NMR spectra for the cycloaddition reaction of styrene oxide using SSICG-6.

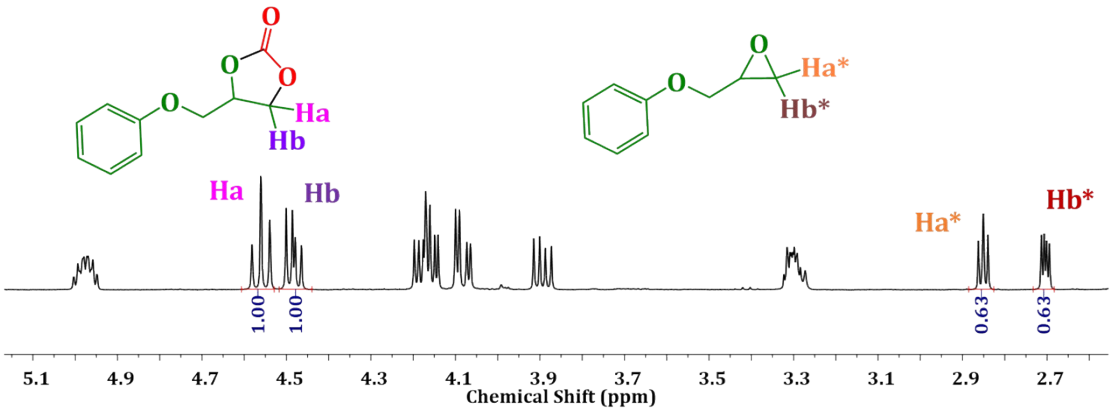

Figure. S13. ^{1}H NMR spectra for the cycloaddition reaction of phenyl glycidyl ether using SSICG-6.

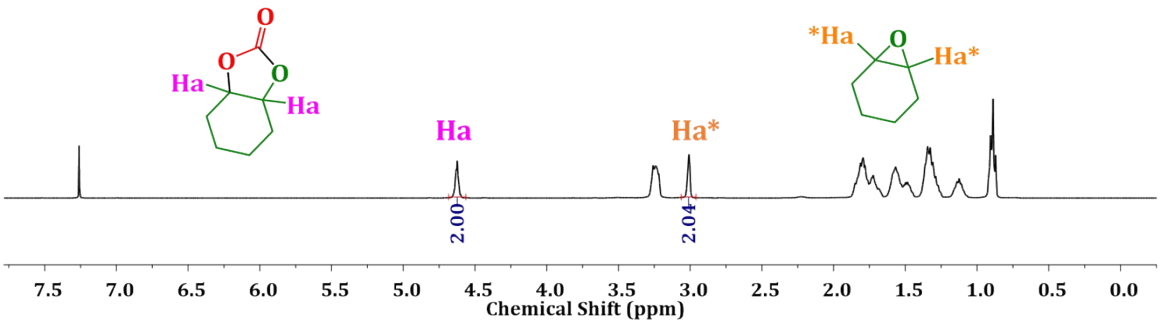

Figure. S14. ^{1}H NMR spectra for the cycloaddition reaction of epoxycyclohexane using SSICG-6.

Table S2. Comparison table for the catalytic performance of SSICG-6 with other reported 1D catalysts for CO_2 cycloaddition reaction.

Entry	Catalyst	Time (h)	Pressure (bar)	Temperature (°C)	Conversion (%)	Ref.
1	$[Yb(\mu\text{-}L)(\mu_3\text{-}L)(H_2O)]_nBr_n$	12	1	70	98	9
2	BIT-C	12	1	35	96	10
3	ADES-3	8	10	80	99	11
4	$ZrCl_4\cdot(OEt_2)_2$ /$SiO_{2\text{-}200}$	18	10	60	98	12
5	Ni-Co-MOF(M)	8	12	80	96	13
6	$Co(XN)(HCOO)_2(H_2O)_2$	12	1	80	99	14
7	**SSICG-6**	**8**	**1**	**rt**	**99**	**This work**

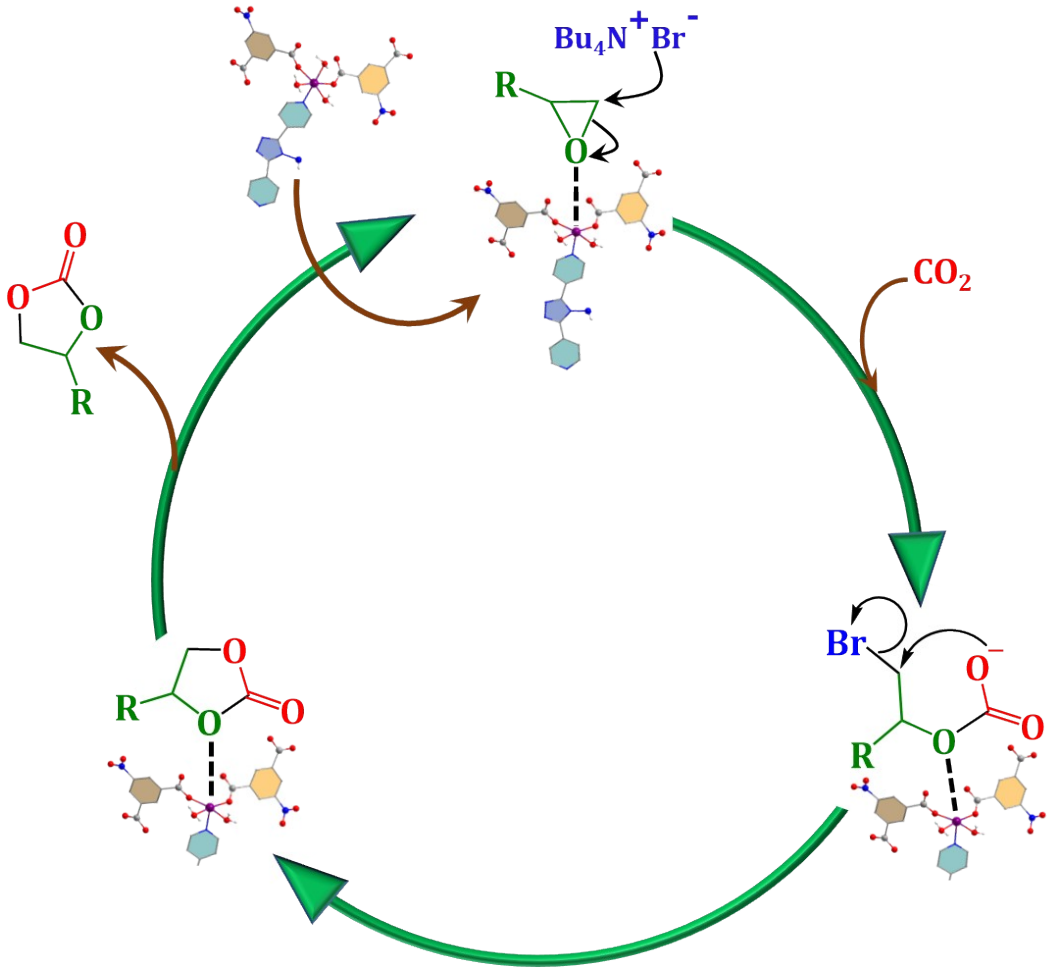

Scheme S1. Plausible mechanism of CO_2 cycloaddition catalyzed by SSICG-6.

Catalytic Hantzsch Condensation

Table S3. Controlled reaction data for the Hantzsch condensation reactions[a]

Entry	Catalyst	Solvent	Temperature (°C)	Time (h)	Conversion (%)
1	$Co(OAc)_2 \cdot 4H_2O$	EtOH	60	6	26
3	H_2NIPA				19
4	4-ABPT				-
5	$Co(OAc)_2 \cdot 4H_2O$ + H_2NIPA + 4-ABPT				29
6[b]	SSICG-6				48
7	-				-
8	SSICG-7			4	98

[a]Reaction condition: benzaldehyde (1 mmol), ethyl acetoacetate (2 mmol), ammonium acetate (1 mmol), solvent (1 mL), catalyst (2.5 mol %).

[b]Catalyst was removed after 30 min.

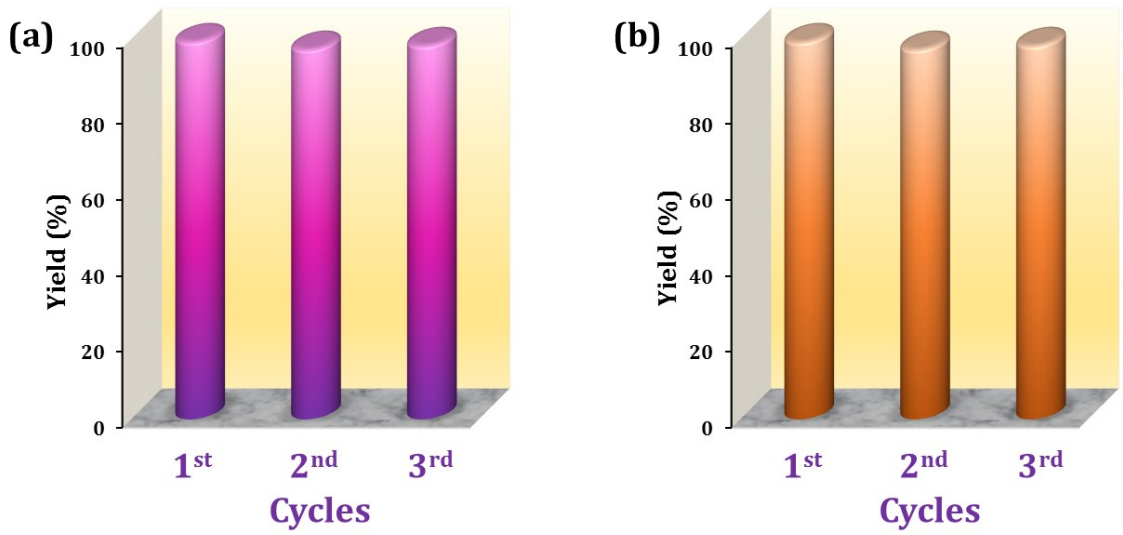

Figure S15. Recyclability test for (a) SSICG-6 and (b) SSICG-7 catalyzed Hantzsch Condensation reaction up to three cycles.

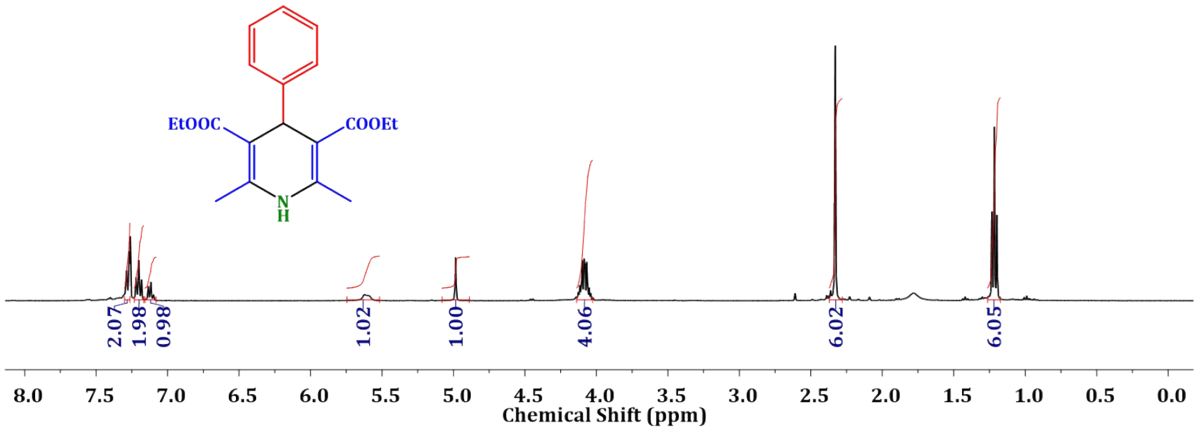

Figure. S16. ^{1}H NMR spectra for 2a.

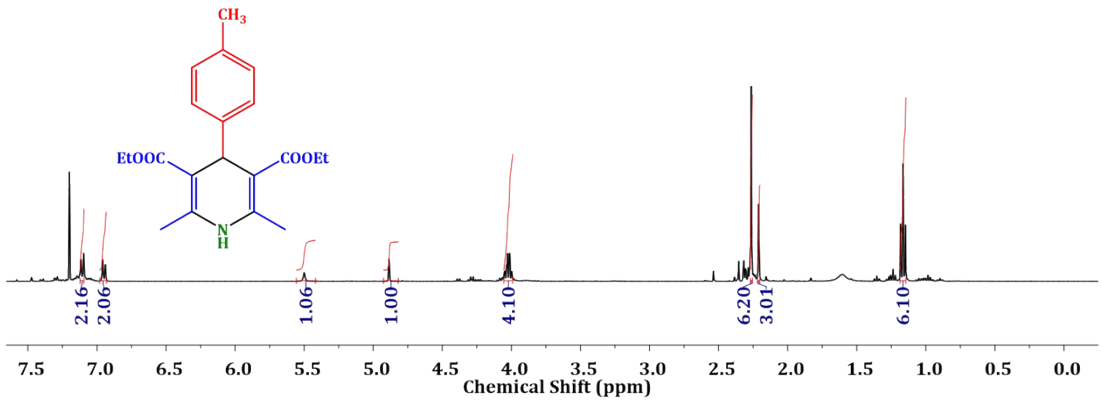

Figure. S17. ^{1}H NMR spectra for 2b.

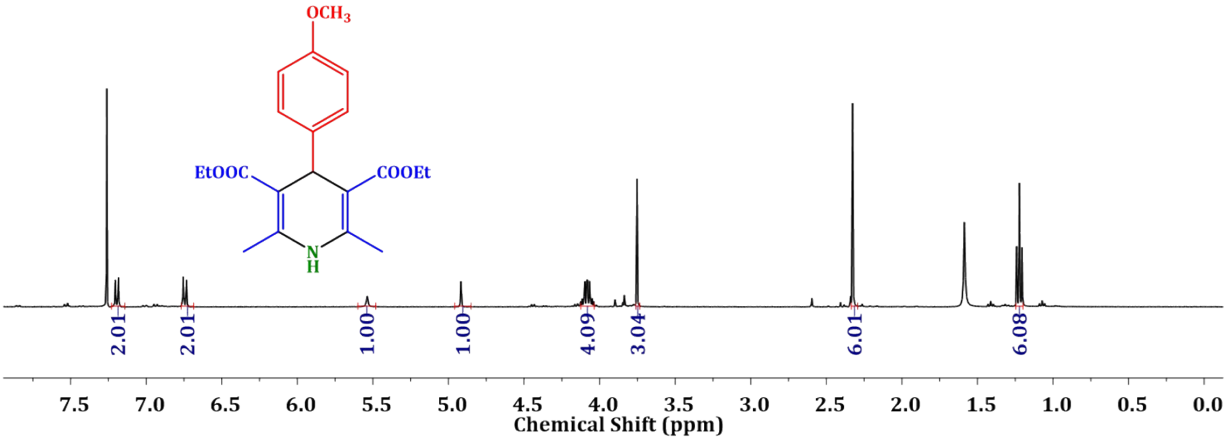

Figure. S18. ^{1}H NMR spectra for 2c.

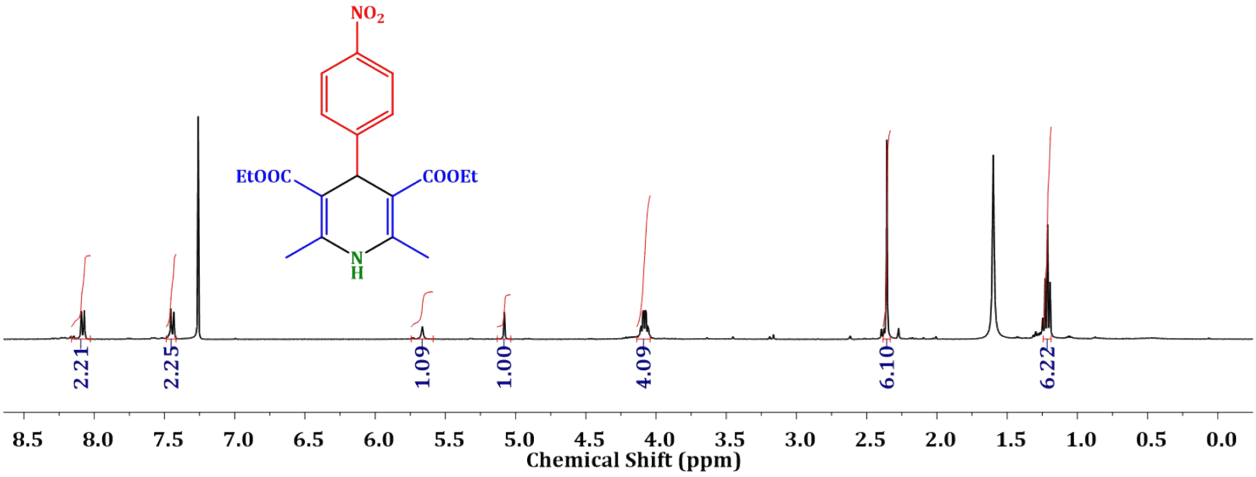

Figure. S19. ^{1}H NMR spectra for 2d.

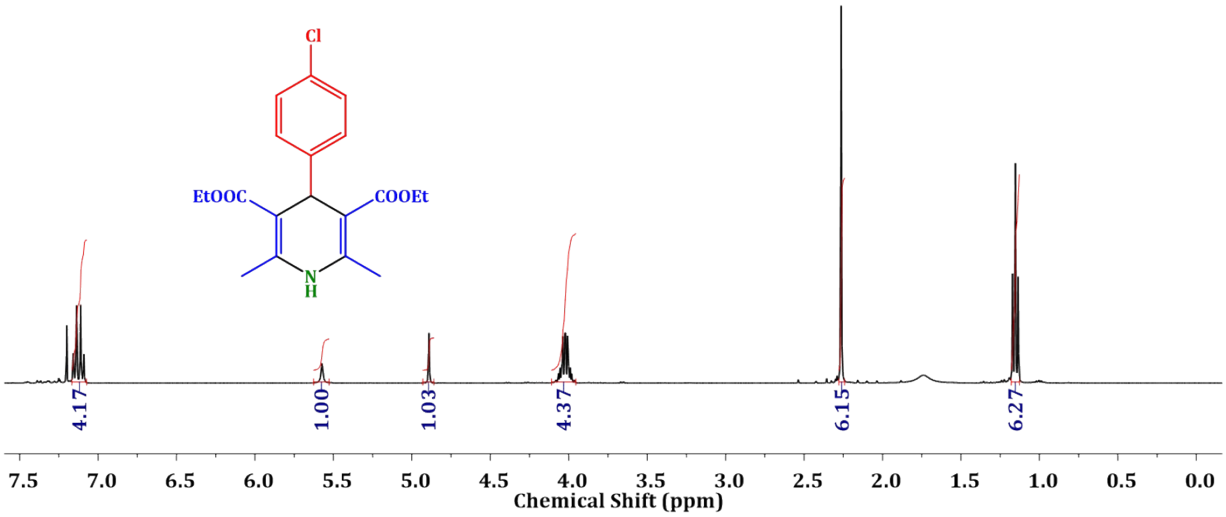

Figure. S20. ^{1}H NMR spectra for 2e.

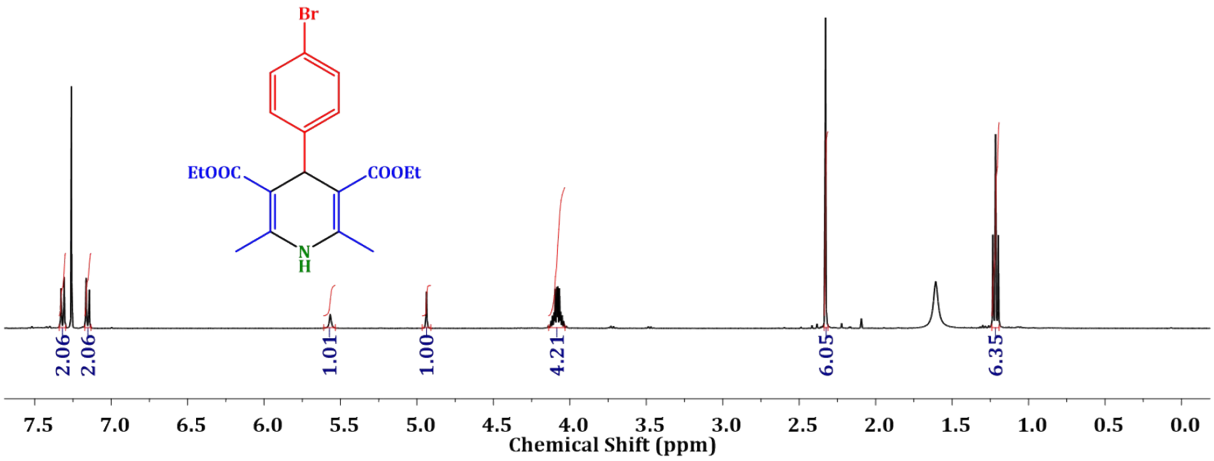

Figure. S21. ^{1}H NMR spectra for 2f.

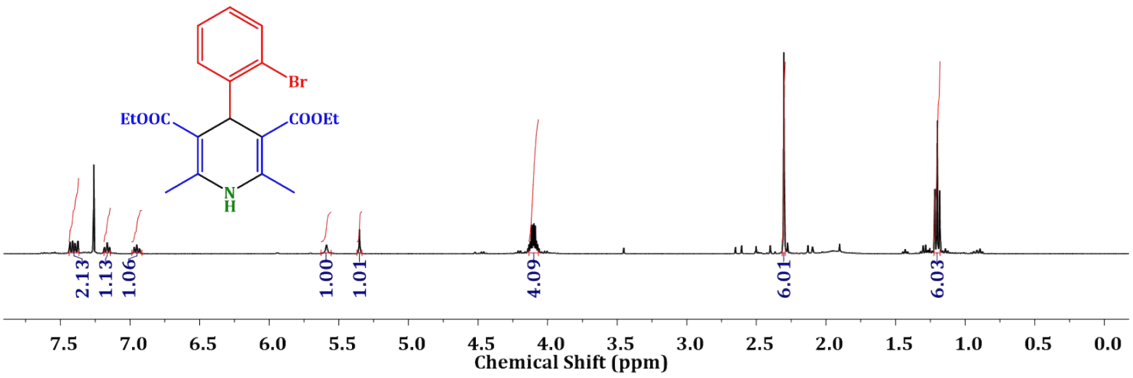

Figure. S22. ^{1}H NMR spectra for 2g.

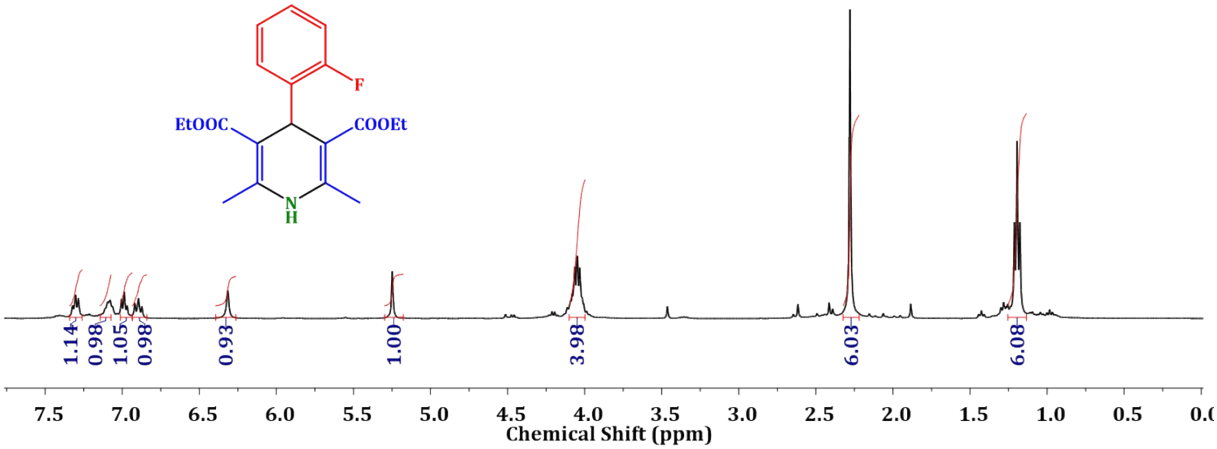

Figure. S23. ^{1}H NMR spectra for 2h.

Table S4. Comparison table for the catalytic Hantzsch condensation performance of SSICG 6- and 7 with other reported catalysts.

Entry	Catalyst	Temp (°C)	Time (h)	Yield (%)	Ref.
1	TMU-33	rt	2	96	[15]
2	Fe-TUD-1	80	5	76	[16]
3	Zr-SBA-16	80	3	77	[17]
4	IRMOF-3	reflux	5	89	[18]
5	Cu(II)-MOF	60	2	98	[19]
6	$Dy(DBM)_3$.bpy	80	5	93	[20]
7	$Cd(H_4L)_{0.5}(4,4';\text{-bpy})_{0.5}(H_2O)_2$	60	4	99	[21]
8	**SSICG-6**	**60**	**4**	**99**	**This work**
9	**SSICG-7**				

Table S5. Selected Bond Distances (Å) and Bond Angles (°)

SSICG-6

Co(1)-O(1)	2.077(5)	Co(1)-O(8)	2.124(5)	Co(1)-O(9)	2.143(5)
Co(1)-O(3)#1	2.119(5)	Co(1)-N(1)	2.134(6)	Co(1)-O(7)	2.150(5)

O(1)-Co(1)-O(3)#1	105.3(2)	O(8)-Co(1)-O(9)	88.7(2)
O(1)-Co(1)-O(8)	89.9(2)	N(1)-Co(1)-O(9)	91.9(2)
O(3)#1-Co(1)-O(8)	89.9(2)	O(1)-Co(1)-O(7)	89.4(2)
O(1)-Co(1)-N(1)	89.7(2)	O(3)#1-Co(1)-O(7)	165.22(19)
O(3)#1-Co(1)-N(1)	89.2(2)	O(8)-Co(1)-O(7)	92.0(2)
O(8)-Co(1)-N(1)	178.8(2)	N(1)-Co(1)-O(7)	89.1(2)
O(1)-Co(1)-O(9)	168.0(2)	O(9)-Co(1)-O(7)	78.73(19)
O(3)#1-Co(1)-O(9)	86.65(19)		

Symmetry transformations used to generate equivalent atoms. #1 -x+1, y-1/2, -z+1/2

SSICG-7

Co(1)-O(1)	2.043(2)	Co(1)-N(6)#1	2.124(3)	Co(1)-N(1)	2.142(3)
Co(1)-O(7)	2.082(2)	Co(1)-O(4)#2	2.135(3)	Co(1)-O(3)#2	2.244(3)
Co(1)-C(8)#2	2.501(4)				

O(1)-Co(1)-O(7)	90.02(10)	O(7)-Co(1)-O(3)#2	87.59(10)
O(1)-Co(1)-N(6)#1	110.93(12)	N(6)#1-Co(1)-O(3)#2	94.41(11)
O(7)-Co(1)-N(6)#1	90.33(11)	O(4)#2-Co(1)-O(3)#2	59.84(10)
O(1)-Co(1)-O(4)#2	95.00(11)	N(1)-Co(1)-O(3)#2	96.98(11)
O(7)-Co(1)-O(4)#2	92.35(11)	O(1)-Co(1)-C(8)#2	124.58(12)
N(6)#1-Co(1)-O(4)#2	153.93(11)	O(7)-Co(1)-C(8)#2	85.72(11)

O(1)-Co(1)-N(1)	87.36(11)	N(6)#1-Co(1)-C(8)#2	124.30(13)
O(7)-Co(1)-N(1)	174.22(12)	O(4)#2-Co(1)-C(8)#2	30.39(11)
N(6)#1-Co(1)-N(1)	85.79(12)	N(1)-Co(1)-C(8)#2	100.01(12)
O(4)#2-Co(1)-N(1)	93.02(12)	O(3)#2-Co(1)-C(8)#2	29.99(10)
O(1)-Co(1)-O(3)#2	154.57(11)		

Symmetry transformations used to generate equivalent atoms. #1 -x+2,y+1/2,-z+1/2; #2 x,-y+3/2,z-1/2

Table S6. H-bonding interactions

SSICG-6

D --H …A	d(H…A) (Å)	D(D…A) (Å)	< DHA (^{O})
N5 --H5B ..O6#1	2.43	2.953(12)	120
O7 --H7A ..O2#2	1.94	2.754(7)	159
O7 --H7B ..N2#3	2.01	2.826(7)	161
O8 --H8A ..O4#4	2.06	2.789(7)	144
O8 --H8B ..O2#2	2.03	2.855(8)	162
O9 --H9A ..N6#5	2.22	2.723(9)	118w
O9 --H9B ..O7	2.39	2.724(7)	104w
O9 --H9B ..O3#1	2.11	2.916(7)	157

Symmetry transformations used to generate equivalent atoms. #1 3/2-x, -1/2+y, z; #2 -1/2+x, y, 1/2-z; #3 3/2-x,1/2+y, z; #4 2-x, -1/2+y,1/2-z; #5 3/2-x, -y, 1/2+z

SSICG-7

D --H …A	d(H…A) (Å)	D(D…A) (Å)	< DHA (^{O})
N5 --H5A ..O2#1	2.43	2.953(12)	120
N5 --H5B ..O4#2	1.94	2.754(7)	159
O7 --H7A ..O2	2.01	2.826(7)	161
O7 --H7B ..N3#3	2.06	2.789(7)	144

Symmetry transformations used to generate equivalent atoms. #1 1-x,-1/2+y,1/2-z; #2 x,1/2-y,1/2+z; #3 1+x,1/2-y,1/2+z

References

1. L. Cheng, W.-X. Zhang, B.-H. Ye, J.-B. Lin and X.-M. Chen, In Situ Solvothermal Generation of 1,2,4-Triazolates and Related Compounds from Organonitrile and Hydrazine Hydrate: A Mechanism Study, *Inorg. Chem.*, 2007, **46**, 1135-1143.
2. C. Zhan, S. Ou, C. Zou, M. Zhao and C.-D. Wu, A luminescent mixed-lanthanide-organic framework sensor for decoding different volatile organic molecules, *Anal. Chem.*, 2014, **86**, 6648-6653.

3. B. Wang, X.-L. Lv, D. Feng, L.-H. Xie, J. Zhang, M. Li, Y. Xie, J.-R. Li and H.-C. Zhou, Highly stable Zr(IV)-based metal–organic frameworks for the detection and removal of antibiotics and organic explosives in water, *J. Am. Chem. Soc.*, 2016, **138**, 6204-6216.
4. G. M. Sheldrick, Siemens area correction absorption correction program, *University of Göttingen, Göttingen, Germany*, 1994.
5. G. M. Sheldrick, SHELXL-97 program for crystal structure solution and refinement, *University of Göttingen, Göttingen, Germany*, 1997.
6. J. L. Farrugia, WinGx suite for small-molecule single crystal crystallography, *J. Appl Crystallogr.*, 1999, **32**, 837.
7. O. V. Dolomanov, L. J. Bourhis, R. J. Gildea, J. A. Howard and H. Puschmann, OLEX2: a complete structure solution, refinement and analysis program, *J. Appl. Crystallogr.*, 2009, **42**, 339-341.
8. L. J. Bourhis, O. V. Dolomanov, R. J. Gildea, J. A. Howard and H. Puschmann, The anatomy of a comprehensive constrained, restrained refinement program for the modern computing environment - Olex2 dissected, *Acta Crystallogr. A: Found. Adv.*, 2015, **71**, 59-75.
9. C. Xu, Y. Liu, L. Wang, J. Ma, L. Yang, F.-X. Pan, A. M. Kirillov and W. Liu, New lanthanide(iii) coordination polymers: synthesis, structural features, and catalytic activity in CO_2 fixation, *Dalton Trans.*, 2017, **46**, 16426-16431.
10. B. Zou, L. Hao, L.-Y. Fan, Z.-M. Gao, S.-L. Chen, H. Li and C.-W. Hu, Highly efficient conversion of CO_2 at atmospheric pressure to cyclic carbonates with in situ-generated homogeneous catalysts from a copper-containing coordination polymer, *J. Catal.*, 2015, **329**, 119-129.
11. U. Patel, P. Patel, B. Parmar, A. Dadhania and E. Suresh, Synergy of Dual Functional Sites for Conversion of CO_2 in a Cycloaddition Reaction under Solvent-Free Conditions by a Zn(II)-Based Coordination Network with a Ladder Motif, *Cryst. Growth Des.*, 2021, **21**, 1833-1842.
12. M. J. Kelly, A. Barthel, C. Maheu, O. Sodpiban, F.-B. Dega, S. V. C. Vummaleti, E. Abou-Hamad, J. D. A. Pelletier, L. Cavallo, V. D'Elia and J.-M. Basset, Conversion of actual flue gas CO_2 via cycloaddition to propylene oxide catalyzed by a single-site, recyclable zirconium catalyst, *J. CO_2 Util.*, 2017, **20**, 243-252.
13. J. F. Kurisingal, R. Babu, S.-H. Kim, Y. X. Li, J.-S. Chang, S. J. Cho and D.-W. Park, Microwave-induced synthesis of a bimetallic charge-transfer metal organic framework: a

promising host for the chemical fixation of CO_2, *Catalysis Science & Technology*, 2018, **8**, 591-600.

14. J.-J. Lv, F.-L. Cao, M.-L. Wang, X.-M. Zong, X.-M. Kang and Z.-L. Wu, A new Co-based metal-organic coordination polymer as a catalyst in chemical fixation of CO_2, *Polyhedron*, 2021, **195**, 114982.
15. F. Rouhani and A. Morsali, Highly effective Brønsted base/lewis acid cooperative catalysis: a new Cd metal–organic framework for the synthesis of Hantzsch 1, 4-DHPs at ambient temperature, *New J. Chem.*, 2017, **41**, 15475-15484.
16. V. V. Srinivasan, M. P. Pachamuthu and R. Maheswari, Lewis acidic mesoporous Fe-TUD-1 as catalysts for synthesis of Hantzsch 1,4-dihydropyridine derivatives, *J. Porous Mater.*, 2015, **22**, 1187-1194.
17. R. Maheswari, V. V. Srinivasan, A. Ramanathan, M. P. Pachamuthu, R. Rajalakshmi and G. Imran, Preparation and characterization of mesostructured Zr-SBA-16: efficient Lewis acidic catalyst for Hantzsch reaction, *J. Porous Mater.*, 2015, **22**, 705-711.
18. S. Rostamnia and A. Morsali, Basic isoreticular nanoporous metal–organic framework for Biginelli and Hantzsch coupling: IRMOF-3 as a green and recoverable heterogeneous catalyst in solvent-free conditions, *RSC Adv.*, 2014, **4**, 10514-10518.
19. N. Seal and S. Neogi, Intrinsic-unsaturation-enriched biporous and chemorobust Cu(II) framework for efficient catalytic CO_2 fixation and pore-fitting actuated size-exclusive hantzsch condensation with mechanistic validation, *ACS Appl. Mater. Interfaces*, 2021, **13**, 55123-55135.
20. A. Sarkar, P. P. Mondal and H. P. Nayek, One-Pot and Solvent-Free Hantzsch Condensation Reaction Catalyzed by Mononuclear Dy(III) Complex, *ChemistrySelect*, 2020, **5**, 12302-12306.
21. R. Sahoo, B. Pramanik, S. Mondal and M. C. Das, A Highly Chemically Robust 3D Interpenetrated MOF Heterogeneous Catalyst for the Synthesis of Hantzsch 1,4-Dihydropyridines and Drug Molecules, *Small*, 2024, 2309281.